Non-contact acoustic cell trapping in disposable glass capillaries

Björn Hammarström,[a] Mikael Evander,[b] Herve Barbeau,[a] Mattias Bruzelius,[a] Jörgen Larsson,[a] Thomas Laurell*[a] and Johan Nilsson[a]

Received 22nd March 2010, Accepted 28th May 2010
DOI: 10.1039/c004504g

Non-contact trapping using acoustic standing waves has shown promising results in cell-based research lately. However, the devices demonstrated are normally fabricated using microfabrication or precision machining methods leading to a high unit cost. In *e.g.* clinical or forensic applications avoiding cross-contamination, carryover or infection is of outmost importance. In these applications disposable devices are key elements, thus making the cost per unit a critical factor. A solution is presented here where low-cost off-the-shelf glass capillaries are used as resonators for standing wave trapping. Single-mode as well as multi-node trapping is demonstrated with an excellent agreement between simulated and experimentally found operation frequencies. Single particle trapping is verified at 7.53 MHz with a trapping force on a 10 μm particle of up to 1.27 nN. The non-contact trapping is proved using confocal microscopy. Finally, an application is presented where the capillary is used as a pipette for aspirating, trapping and dispensing red blood cells.

Introduction

Non-contact trapping/retention of particles and cells in microfluidic systems has emerged as a powerful approach to detailed cell–compound and cell–cell interaction studies. The developments have taken a clear route towards lab-on-a-chip solutions where the well-controlled microenvironment and the ability to design parallel systems for screening and population-based studies are key factors. The literature describes a wealth of techniques for cell trapping where biological preconditions are maintained to enable cell-based studies of extended time periods.[1] The most common non-contact trapping techniques are optical tweezers,[2–4] dielectric trapping[5–7] and acoustic trapping.[8–10] These are all suited for cell-based experiments offering trapping forces up to a few 100 pN.

In acoustic trapping an acoustic standing wave is generated in a channel or a cavity. The trapping force is related to the density and compressibility difference between the object and the surrounding media. Thus there is no demand on transparent properties or optical access. The method is also compatible with almost all beads available off-the-shelf today for bead-based chemistry. Acoustic trapping has been demonstrated in: (a) layered resonator structures[11,12] manufactured using precision machining; (b) microfabricated in-channel transducer structures with a glass lid incorporating the microchannel[9,13–14] and (c) microfabricated resonant cavity structures with external transducers.[15–18] All the acoustic trapping methods have been demonstrated in connection with cell experiments.[9,16,17,19–21] A further benefit of acoustic trapping is that the external instrumentation needed is simple, in principle an electronic waveform generator.

So far, the presented methods are based on device designs that require access to either precision machining or microfabrication facilities. The final cost per unit will then be quite high. In several applications within biology, such as clinical diagnosis and forensics, there is a clear need for disposable devices to completely avoid carryover or infection. In such applications the presented methods are hardly suited due to the device costs involved. Polymer devices are often used as the solution to minimize the costs. Here, the start-up cost is quite high but the cost per unit at the end is low when the volumes get reasonably large. Unfortunately, polymer-based devices commonly perform poorly in terms of intrinsic mechanical properties and are normally not possible to use in connection with acoustically resonant systems. The high losses in the materials in combination with the low difference in acoustic impedance between water and the polymer lead to a low *Q*-value resonator and thus a strong resonance defined by the microstructure design will not be achieved.

Pre-made glass capillaries with mm-sized circular or square cross-section have earlier been used for acoustic particle manipulation in agglutination experiments.[22,23] Ultrasound was applied to the capillaries by a relatively large ring-shaped transducer (31.5 mm diameter, 20 mm long) using water as coupling medium. The capillaries were loaded with sample droplets separated with air and the ultrasound was used to concentrate the particles or cells in the stationary fluid to enhance the agglutination tests. The length and diameter of the transducer, the large water container and the fact that the transducer surrounds the capillary preventing easy optical access makes the set-up impractical to use for trapping purposes.

This paper reports a promising solution, using low-cost off-the-shelf disposable flat glass capillaries as acoustic resonators (Fig. 1) for cell or particle trapping in a flowing liquid. In contrast to previously reported chip microfabricated acoustic trapping devices that are only justified in systems of reuse, the disposable glass capillary platform opens the route to implement acoustic trapping as a modality in automated high throughput systems where single use is fundamental requirement in applications such as diagnostics, forensics and screening operations.

The breakthrough is given by the ability to localize an acoustic field in a flat capillary by simply docking the capillary to

[a]*Dept. of Measurement Technology and Industrial Electrical Engineering, Div. Nanobiotechnology, Lund University, Lund, Sweden. E-mail: thomas.laurell@elmat.lth.se; Fax: +46 46 2224527; Tel: +46 46 2227540*
[b]*Dept. of Electrical Engineering, Stanford University, CA, USA*

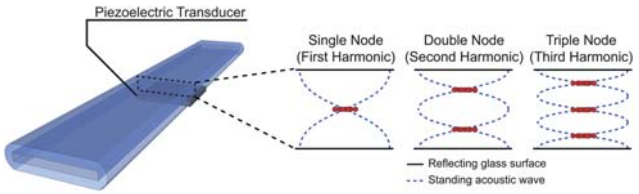

Fig. 1 A rectangular borosilicate capillary is contacted with a piezo-electric transducer. When actuation matches the resonance criteria in the capillary a localized standing wave is formed above the transducer. Operation at the first, second and third harmonics corresponds to trapping at one, two or three nodes.

a reusable printed circuit board carrying integrated air-backed piezo-electric transducers. By connecting the capillaries to a syringe pump an aspirate–dispense pipette system with non-contact trapping has for the first time been developed. The system was evaluated in terms of capillary resonance reproducibility and obtained trapping force. COMSOL modelling verified the observed non-contact single node and triple node trapping localisation in all three dimensions. The first acoustic cell trapping in an aspirate and dispense mode using the disposable glass capillary is also reported.

Materials and methods

Acoustic forces and pressure gradients

Acoustic trapping in microfluidic systems commonly employs an ultrasonic standing wave localized to a confined region of a microchannel. For spherical incompressible particles smaller than the wavelength the primary acoustic force has been thoroughly equated by King,[24] Gorkov[25] and Gröschl.[26] A force expression based solely on the pressure field from the original force equation by Gorkov[25] was recently derived by Manneberg *et al.*[27]

$$F = -\frac{V\beta}{2}\left[\left(1-\frac{\beta_p}{\beta}\right)p\nabla p - \frac{3}{k^2}\left(\frac{\rho_p-\rho}{2\rho_p+\rho}\right)(\nabla p\times\nabla)\nabla p\right] \quad (1)$$

where, V is the particle volume, ρ and ρ_p are the densities of the media and the particle, β and β_p are the compressibilities of the media and particle, k is the wave number in the medium and p is the pressure distribution field. The relation between the particle and media density and sound velocity dictates the direction of the primary acoustic radiation force. In an aqueous medium the force commonly drives cells and particles with higher density and lower compressibility relative to the buffer into the pressure minima.[28]

Acoustic trapping manifold

Non-contact acoustic cell trapping was performed in single-use rectangular channel borosilicate capillaries (Virtrotubes, VirtroCom, New Jersey, USA) of three different internal dimensions: 100 × 1000 μm, 100 × 2000 μm and 200 × 2000 μm. The capillaries were upstream connected to 1/16″ Teflon-tubing by attaching a 1 cm long silicone-tubing to the capillary with silicone glue.

The capillaries were clamped *via* a cross-shaped polymethyl methacrylate (PMMA) holder to three 10 MHz piezoelectric transducers (PZ26, Ferroperm Piezoceramics, Kvistgard, Denmark) integrated on a printed circuit board (PCB) (Fig. 2). Air-backing of the transducers (Fig. 3) and a sufficient pressure from the PMMA clamp ensured good acoustic coupling between transducer and capillary. The PMMA clamp was supplied with a milled trench to ensure reproducible mounting of the capillaries over the transducers. The bottom of the trench was supplied with a thin polydimethylsiloxane film to provide an even pressure distribution, avoiding breakage of the capillary. A square opening in the centre of the cross-shaped PMMA clamp enables optical access to the trapping sites above the transducers. This manifold design enables simple exchange of capillaries between each experiment while using the same transducer board.

The three 900 × 900 μm^2 transducers were diced from a single 5 mm diameter 10 MHz transducer and mounted on the PCB using conductive silver epoxy (Fig. 3). Electrical wiring to the transducer was formed by removal of copper from the PCB surface through a standard milling process. Holes for air-backing of the transducers were drilled in the PCB. The transducer board was turned face down against a Teflon covered surface and cast in epoxy. After polishing this provides a planar surface to dock the capillaries against the transducer array. To form a ground contact

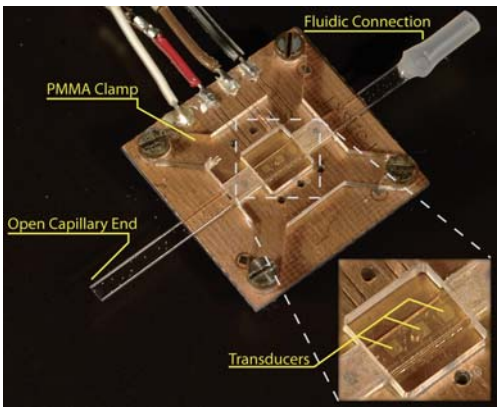

Fig. 2 Manifold for acoustic trapping in borosilicate capillaries. Three miniature transducers are mounted on a PCB and cast in epoxy. The capillary is clamped to the chip with a PMMA holder. Acoustic contact between transducer and capillary is provided by a thin layer of glycerol.

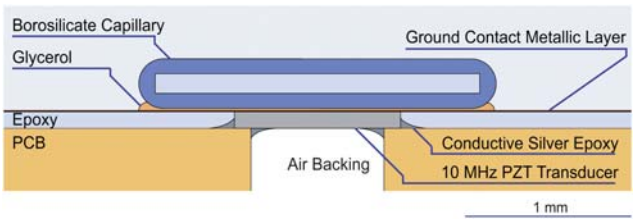

Fig. 3 A two-scale cross-section schematic of the capillary and transducer board used in the acoustic trapping manifold. The 10 MHz PZT element is contacted on both sides using silver epoxy and an evaporated silver or gold layer, glycerol is used as an acoustic coupling layer. Furthermore, drilled holes beneath the transducer provide air-backing needed for good acoustic coupling.

to the transducers a thin gold or silver layer was deposited by evaporation.

Before clamping the capillary a drop of glycerol was applied to the transducer with the tip of a needle. Upon clamping, the glycerol formed a thin layer between capillary and transducer, providing acoustic contact. Glycerol was chosen as a contact agent since its hygroscopic properties allowed extended periods of continuous operation.

Operation frequencies

The capillaries can be operated at frequencies corresponding to the first vertical resonance and its overtones. Operation at the first harmonic will trap one cluster in the centre of the channel while operation at the higher order harmonics will trap two or more vertically aligned clusters. This is termed single and multiple node trapping (*cf.* Fig. 1).

For each experiment a separate capillary was used. Since the dimensions of the capillaries vary (±10%, according to the specifications) each will have a unique set of operation frequencies giving rise to non-contact trapping.

A large number of capillaries were evaluated with respect to suitable operation frequencies for single- and multiple-node trapping. This was performed by manually scanning for resonance conditions suitable for trapping of 5 μm polyamide beads in a moderate flow (5 μL min^{-1}). This was done within the 2–16 MHz range considered reasonable for the transducers used.

Resonance modelling

To enable prediction of suitable operation frequencies without manual tuning a simulation model is proposed. Considering that no reflective surfaces are present in the flow direction a 2D cross-sectional model is proposed where the Eigen-modes to the Helmholtz equation are calculated using the COMSOL acoustics module.[29,30] In COMSOL, two sub-domains are defined, one for the liquid medium and one for the borosilicate glass. The outer edge of the glass is regarded as a free boundary.

To validate the model, a contour trace from a micrograph of the open end of a 100 × 2000 μm capillary was used to define geometrical dimensions for the cross-section simulation. As can be seen from the cross-section image, the capillary walls show a slight curvature due to the manufacturing process. This will have a noticeable effect on the operation frequency and thus making a simpler parallel walls approximation inadequate. Based on the contour trace geometry the Eigen-frequencies corresponding to the first and second vertical resonances were calculated. The calculated values were compared to the trapping frequencies found manually for the capillary.

Single particle trapping force

The trapping force exerted on a cell or particle is important since it sets the limit for fluidic throughput and speed at which a system can be operated. In general, a system with high trapping force is reliable in terms of tolerance to flow fluctuations. Furthermore, the trapping strength is useful as a means of comparison with alternative trapping techniques.[1]

At low Reynolds numbers, characteristic for microfluidic flow, Stoke's law governs the fluidic drag force.

$$F = 6\pi\eta r v$$

Here, η is fluid viscosity, r particle radius and v fluid velocity. If the flow is gradually increased a single particle trapping force can be calculated by equating the fluidic drag force to the trapping force just prior to overcoming it.[9]

The trapping strength was evaluated for the 100 × 2000 μm capillaries by trapping a single 10 μm polystyrene bead from a highly diluted solution. The capillary was actuated with 7 V peak-to-peak at 7.53 MHz. This drive voltage has been shown not to cause any excessive heating in previous work.[9] Fluid flow was successively increased in 1 μL min^{-1} steps until displacing the particle from the trap. The fluidic drag was calculated from the flow rate by using the capillary centre velocity as calculated using COMSOL.

Cluster conformation and positioning

To evaluate particle cluster conformation in the capillary confocal microscopy was used. A cluster composed of 4.2 μm fluorescein isothiocyanate (FITC) tagged polystyrene beads was trapped under a 10 μL min^{-1} perfusion in a 100 × 2000 μm capillary at 7.69 MHz actuation. Several consecutive confocal scans ranging from the top to the bottom of the capillary were recorded with an Olympus BX51WI microscope. These were used for a volume reconstruction to visualize the cluster conformation using Fluoview 300 software. During the confocal scan the flow was temporarily stopped to reduce image distortion from flow pulsations.

Erythrocyte trapping

The system was demonstrated as an aspirate and trap device for cell-based experiments (Fig. 4) where acoustic trapping of erythrocytes were performed. A 1 μL drop of whole blood was diluted ten times with phosphate buffered saline (PBS). The diluted blood was aspirated into a 200 × 2000 μm capillary using a syringe pump whereupon erythrocytes were trapped using a 10.8 MHz triple-node actuation. Reversing the flow using a running buffer of PBS expelled excess cells and plasma, only leaving cells in the acoustic trapping zone.

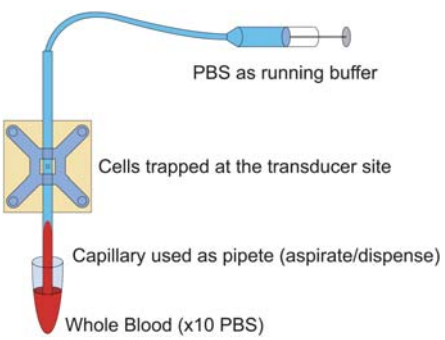

Fig. 4 The trapping capillary is used as a pipette where cells and analyte can be aspirated and deposited in regular Eppendorf tubes while fluid flow is controlled with a syringe pump. Here, diluted whole blood is aspirated (1), a cluster is trapped (2) and flow is reversed (3) expelling excess cells and plasma, washing the cells with PBS.

Instrumentation

Throughout the experiments the following equipments were used: a Hewlett-Packard 3325B waveform generator and a T&C Power Conversion Inc., AG 1020 amplifier for actuation, a World Precision Instruments Inc., SP210IWZ syringe pump for fluid control and a NIKON SMZ-1000 optical stereo microscope for standard microscopy.

Results and discussion

Operation frequencies

Frequency distribution charts for the three capillary dimensions evaluated in the study are shown in Fig. 5. The operation frequencies are divided into 100 kHz bins corresponding to the average tolerance for frequency tuning. These data provide a good basis for choosing a starting point for manual frequency tuning. As is evident from the graph up to four modes of operation are available within the frequency range tested, corresponding to the vertical resonance modes of the different set-ups (*cf.* Fig. 1).

Frequency simulations

The capillary used for contour tracing was measured using optical microscopy (Fig. 6). This resulted in inner and outer dimensions of 122.4 × 2073.07 μm and 344.7 × 2260.8 μm respectively. The contour trace was adjusted to these dimensions before entering it into the simulations software. Running the simulations model gave first and second harmonics for the vertical modes at 6.71 MHz and 12.48 MHz (*cf.* Fig. 6). Compared to the optimal operation frequencies found experimentally for this capillary at 6.78 MHz and 12.52 MHz, this shows that the frequency can be predicted within the 100 kHz range.

Simulation of the first harmonic clearly shows the pressure node located in the channel centre used for trapping a single cluster and the second harmonic shows the two corresponding nodes used for double node trapping. In comparison to a parallel wall model, simulations show that accounting for the slight wall curvature results in an improved frequency prediction as well as a laterally confined pressure pattern. The laterally confined pressure pattern is in good agreement with the experimental observations where the cluster is centred both laterally and vertically (*cf.* eqn (1), Fig. 6 and 9).

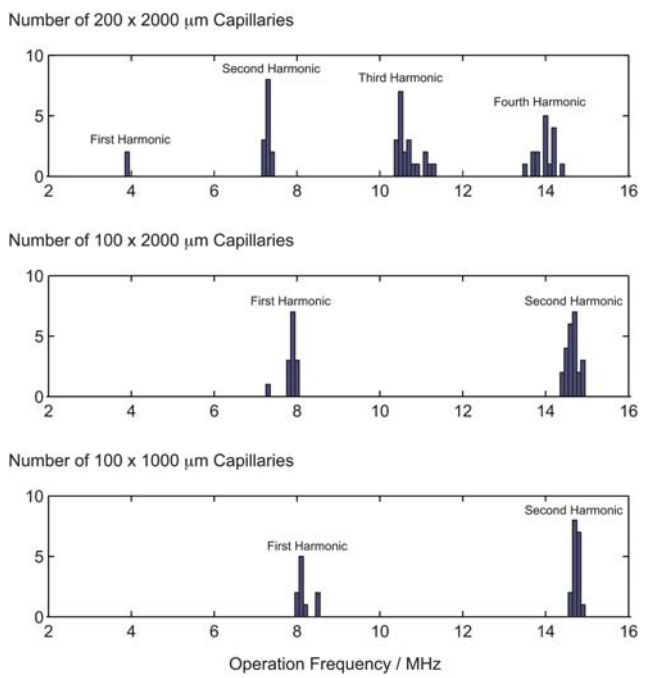

Fig. 5 A frequency distribution chart showing the available modes for trapping in the 2–16 MHz range for a number of glass capillaries of dimensions 200 × 2000 μm, 100 × 2000 μm and 100 × 1000 μm. The resonance frequencies are divided into 100 kHz bins corresponding to the tolerance for frequency tuning.

Single particle trapping force

Evaluating the maximum retention force for a single 10 μm polystyrene bead at a set peak-to-peak voltage of 7 V yielded a force of 1.27 ± 0.11 nN (data from four consecutive runs), corresponding to a flow velocity of 13.4 ± 1.2 mm s^{-1}. In comparison with previously reported acoustic trapping forces at similar actuation frequencies and amplitudes this correspond to more than a factor two increase.[9] Furthermore, the trapping force is on a par with that of optical tweezers.[1]

Cluster conformation and position

In order to evaluate handling of larger groups of cells or microparticles, cluster formation was investigated using confocal microscopy. A 3D reconstruction of trapped fluorescent beads is shown in Fig. 7. The green channel shows fluorescence from the trapped beads and the red channel shows reflective data from the incident laser. The confocal reconstruction shows the 3D distribution in the acoustic trap and clearly confirms non-contact type of trapping, which is in agreement with the results obtained by simulation (*cf.* Fig. 6).

Fig. 8 shows a layered cluster of 10 μm beads trapped above the piezoelectric transducer. The non-contact mode is here confirmed by the light red toned shadow at the lower surface of the capillary. The inset image shows beads arranged in a hexagonal close packed fashion, which illustrates a monolayer at the edges of the trap and multiple layers at the centre.

Erythrocyte trapping

A trapped erythrocyte cluster is shown in Fig. 9a, demonstrating an aspirate–capture–release sequence from ×10 PBS diluted blood. Diluted blood was aspirated into the capillary and cells were trapped in a non-contact fashion upon reaching the active transducer zone. Subsequently, the flow was reversed and untrapped cells outside the trapping zone and plasma were removed and replaced with PBS running buffer, leaving a red elliptic shaped cluster of trapped cells above the transducer. The experiment was operated in a triple node mode (10.8 MHz triple-node actuation of a 200 × 2000 μm capillary), which is seen in the difference in flow velocity of the cells in their respective nodal planes as the ultrasonic actuation is turned off, Fig. 9b. With this experiment, a pipette-like system based on aspiration is

demonstrated where non-contact ultrasonic trapping is included as an added feature.

Conclusions

In summary, we present a novel approach to contactless acoustic trapping that provides a significant device simplification making clean-room micro-fabrication obsolete. Readily available glass capillaries in combination with accurate operation frequency prediction realize the disposable device concept. As disposable devices are key in most biological applications targeted towards forensics or clinical use, this novel approach opens the path for a broad range of uses for acoustic trapping in bioanalytics.

The reported characterization confirms non-contact type of trapping and demonstrates handling of single cells as well as large agglomerates. The possibility of choosing different capillary dimensions in conjunction with the aspiration/dispense based fluidic set-up enables a highly versatile method that can be applied in fields such as cell-based bioassays,[31] cell enrichment and extraction from complex media[19] or 3D positioning in solution for high-resolution microscopy.[17]

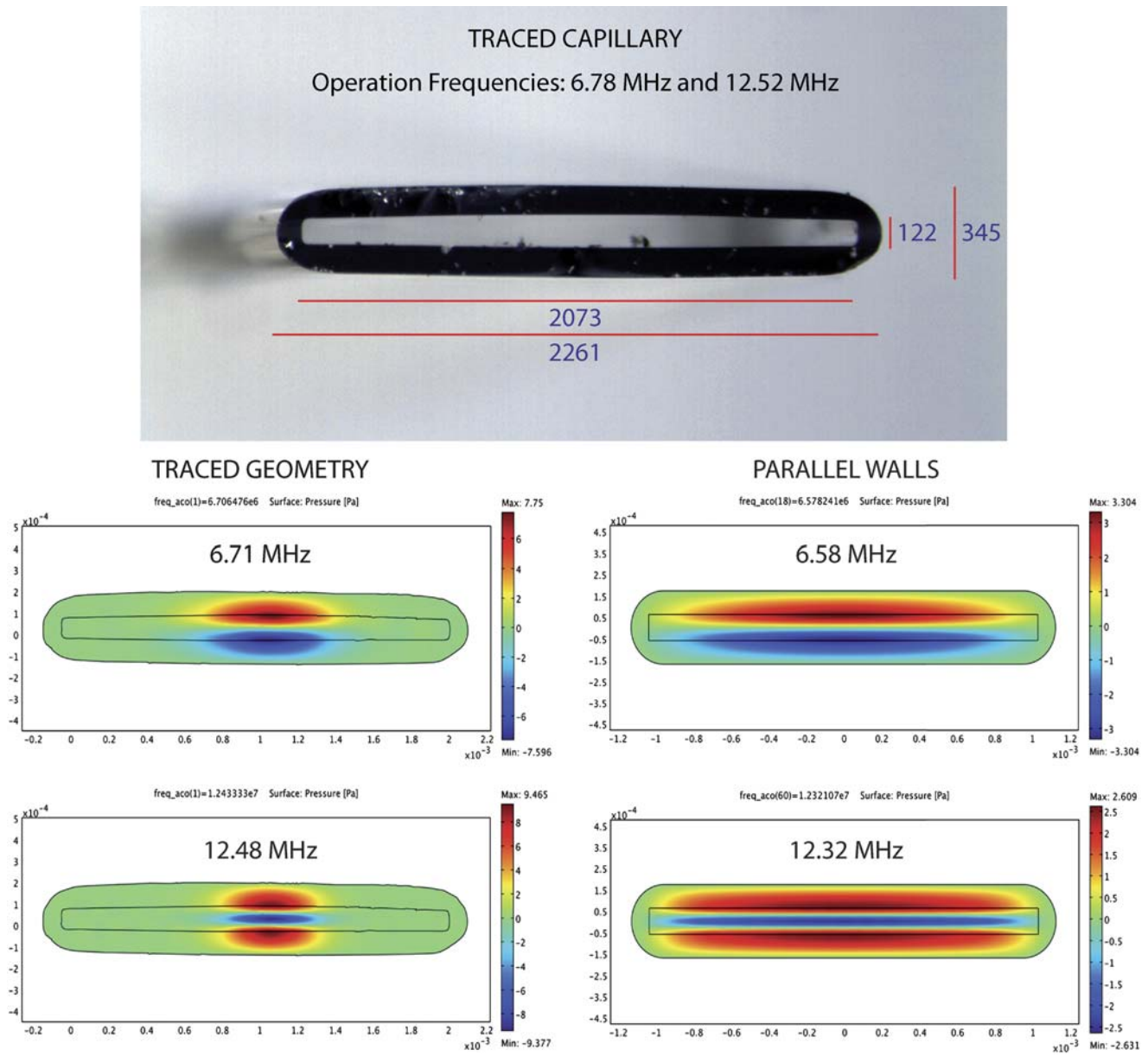

Fig. 6 Cross-sectional simulations show the pressure distribution from the standing ultrasonic wave. Locations where the absolute pressure is close to zero will work as trapping zones. Here, the modes for single and double node trapping in a 100 × 2000 μm capillary are displayed. Comparison between the traced cross-section and the parallel walls assumption (adjusted to the same measures) shows a significantly better frequency prediction for the traced geometry. Furthermore, the acoustic field is localized to the centre of the channel to a greater extent in the traced geometry, which is in concurrence with experimentally observed cluster positioning.

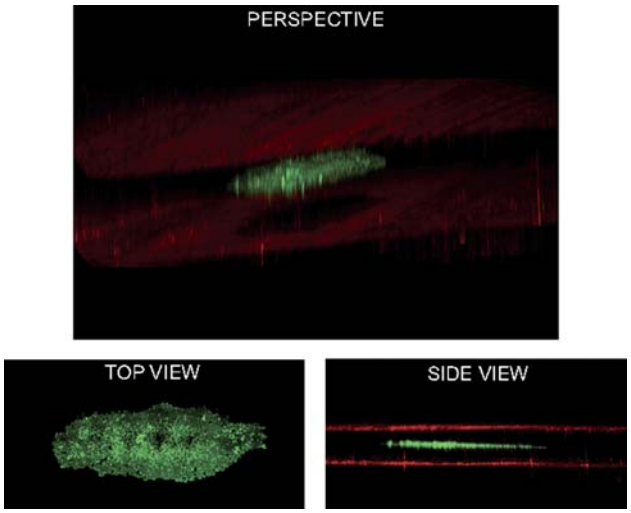

Fig. 7 Confocal reconstruction showing a 3D perspective image of trapped 4.2 μm FITC beads. Green correspond to the FITC fluorescence from the trapped cluster and red is reflective data from the laser showing the upper and lower capillary surfaces. A shadow from the trapped cluster can be seen in the reflective data from of the lower capillary surface. Lower left shows a top view of the trapped cluster and lower right shows a side view of the trapped beads (green) and the capillary walls (red).

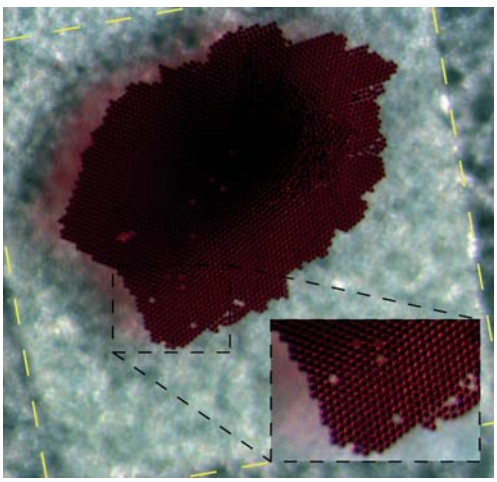

Fig. 8 Detail of trapped 10 μm beads showing the red beads trapped in the centre of the channel, indicated by the light red shadow. The inset image shows that the microbeads form a hexagonally close packed monolayer, including a few dislocations. An outline of the transdducer is indicated by the dashed yellow line.

The trapping forces presented here are high in comparison with previously reported values for acoustic trapping and even on par with those reported for optical trapping.[1] This opens up for reasonable aspirate/trap/release cycles in sequences where cells can be exposed to chemical stimuli of predefined concentration and period of time. Also, an outlook towards a parallel configuration in a microtiter well-plate format will enable implementation of the platform in *e.g.* screening assays for non-adherent cells.

Finally, the reported system opens up for in-depth cell–drug and cell–cell interaction studies where sterile conditions are required or where avoiding system carryover is critical for the analytical readout.

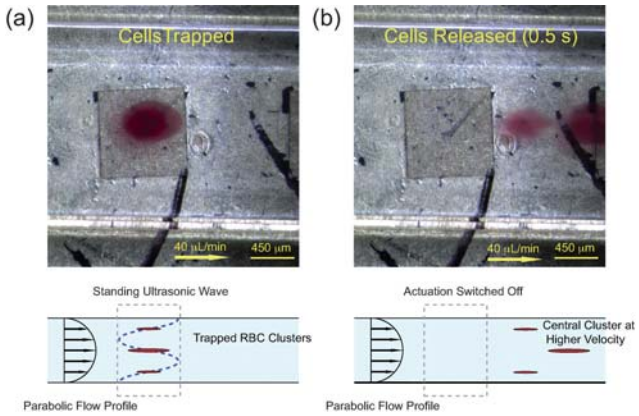

Fig. 9 (a) Three vertically aligned erythrocyte clusters are held against a fluid flow of 40 μL min^{-1} above the piezoelectric transducer in a non-contact fashion. The red blood cells are trapped from diluted whole blood aspirated into the capillary and upon reversion of the flow only cells above the transducer are retained in the channel. (b) Image taken 0.5 s after switching off the transducer, the cells are released and follows the fluid flow. Here, the cluster positioned in the centre of the channel can be seen outrunning the other two in concurrence with the parabolic flow profile.

Acknowledgements

The authors acknowledge the support from: The Swedish Research Council Project no: 2007–4946; Vinnova programme: Innovation for Future Health—Cell CARE, Foundation for Strategic Research, Crafoordstiftelsen, Carl Trygger Foundation, Royal Physiographic Society in Lund, and Knut & Alice Wallenberg Foundation are greatly acknowledged for their financial support.

References

1 J. Nilsson, M. Evander, B. Hammarstrom and T. Laurell, *Anal. Chim. Acta*, 2009, **649**, 141–157.
2 A. Ashkin, *Phys. Rev. Lett.*, 1970, **24**, 156–159.
3 J. R. Moffitt, Y. R. Chemla, S. B. Smith and C. Bustamante, *Annu. Rev. Biochem.*, 2008, **77**, 205–228.
4 C. Piggee, *Anal. Chem.*, 2009, **81**, 16–19.
5 T. Schnelle, R. Hagedorn, G. Fuhr, S. Fiedler and T. Muller, *Biochim. Biophys. Acta, Gen. Subj.*, 1993, **1157**, 127–140.
6 J. Voldman, M. Toner, M. L. Gray and M. A. Schmidt, *J. Electrost.*, 2003, **57**, 69–90.
7 B. M. Taff and J. Voldman, *Anal. Chem.*, 2005, **77**, 7976–7983.
8 M. Wiklund and H. M. Hertz, *Lab Chip*, 2006, **6**, 1279–1292.
9 M. Evander, L. Johansson, T. Lilliehorn, J. Piskur, M. Lindvall, S. Johansson, M. Almqvist, T. Laurell and J. Nilsson, *Anal. Chem.*, 2007, **79**, 2984–2991.
10 M. Wiklund, C. Gunther, R. Lemor, M. Jager, G. Fuhr and H. M. Hertz, *Lab Chip*, 2006, **6**, 1537–1544.
11 J. F. Spengler and W. T. Coakley, *Langmuir*, 2003, **19**, 3635–3642.
12 D. Bazou, L. A. Kuznetsova and W. T. Coakley, *Ultrasound Med. Biol.*, 2005, **31**, 423–430.
13 T. Lilliehorn, U. Simu, M. Nilsson, M. Almqvist, T. Stepinski, T. Laurell, J. Nilsson and S. Johansson, *Ultrasonics*, 2005, **43**, 293–303.
14 T. Lilliehorn, M. Nilsson, U. Simu, S. Johansson, M. Almqvist, J. Nilsson and T. Laurell, *Sens. Actuators, B*, 2005, **106**, 851–858.
15 M. Evander, Ph.D. Thesis, Lund University, 2008.

16 J. Hultstrom, O. Manneberg, K. Dopf, H. M. Hertz, H. Brismar and M. Wiklund, *Ultrasound Med. Biol.*, 2007, **33**, 145–151.
17 O. Manneberg, B. Vanherberghen, J. Svennebring, H. M. Hertz, B. Önfelt and M. Wiklund, *Appl. Phys. Lett.*, 2008, **93**, 063901–063903.
18 J. Svennebring, O. Manneberg, P. Skafte-Pedersen, H. Bruus and M. Wiklund, *Biotechnol. Bioeng.*, 2009, **103**, 323–328.
19 J. V. Norris, M. Evander, K. M. Horsman-Hall, J. Nilsson, T. Laurell and J. P. Landers, *Anal. Chem.*, 2009, **81**, 6089–6095.
20 G. O. Edwards, W. T. Coakley, J. R. Ralphs and C. W. Archer, *Eur. Cells Mater.*, 2010, 1–12.
21 D. Bazou, E. J. Blain and W. T. Coakley, *Mol. Membr. Biol.*, 2008, **25**, 102–114.
22 M. A. Grundy, W. E. Bolek, W. T. Coakley and E. Benes, *J. Immunol. Methods*, 1993, **165**, 47–57.
23 M. A. Sobanski, C. R. Tucker, N. E. Thomas and W. T. Coakley, *Bioseparation*, 2000, **9**, 351–357.
24 L. V. King, *Proc. R. Soc. London, Ser. A*, 1934, **147**, 212–240.
25 L. P. Gorkov, *Sov. Phys. Dokl. (Engl. Transl.)*, 1962, **6**, 773–775.
26 M. Groschl, *Acustica*, 1998, **84**, 432–447.
27 O. Manneberg, J. Svennebring, H. M. Hertz and M. Wiklund, *J. Micromech. Microeng.*, 2008, **18**, 095025.
28 L. Gherardini, C. M. Cousins, J. J. Hawkes, J. Spengler, S. Radel, H. Lawler, B. Devcic-Kuhar and M. Groschl, *Ultrasound Med. Biol.*, 2005, **31**, 261–272.
29 S. M. Hagsater, T. G. Jensen, H. Bruus and J. P. Kutter, *Lab Chip*, 2007, **7**, 1336–1344.
30 S. M. Hagsater, A. Lenshof, P. Skafte-Pedersen, J. P. Kutter, T. Laurell and H. Bruus, *Lab Chip*, 2008, **8**, 1178–1184.
31 M. Evander, K. Mileros, C. Högberg, D. Erlinge, M. Almqvist, T. Laurell and J. Nilsson, *Proceedings of μTAS 2007 the 11th International Conference on Miniaturized Systems for Chemistry and Life Sciences*, Paris, France, 2007, pp. 1372–1374.